High-resolution angular-resolved measurements of the fragmentation of the core-excited OCS molecule

P. Erman,[1] A. Karawajczyk,[1] E. Rachlew,[1] M. Stankiewicz,[2] and K. Yoshiki Franzén[1]
[1]*Physics Dept. I, Royal Institute of Technology, S-10044 Stockholm, Sweden*
[2]*Instytut Fizyki, Uniwersytet Jagielloński, ulica Reymonta 4, 30-059 Kraków, Poland*
(Received 23 December 1996)

The sulfur $2p$ and carbon $1s$ core-electron excited states of the OCS molecule have been studied in high-resolution angular-resolved photoion experiments. Vibrationally resolved total ion yield spectra of this molecule have been recorded and several previously unobserved states have been revealed and tentatively assigned to the singly excited ns, np, and nd Rydberg levels. The LS-split $\pi^*_{1/2}$ and $\pi^*_{3/2}$ states show significant bond length changes observed as very different intensity distributions of vibrational progressions of these states. Variations of the bond lengths of the Rydberg states have also been revealed by analyzing their vibrational structure. However, in the latter case the effect is found to be mainly dependent on the symmetry of the Rydberg electron orbital, while the state of the core electron plays a minor role. Asymmetric dissociation from the core-excited levels has been studied using the angular-resolved photoelectron-photoion technique. In general the derived values of the asymmetry parameters β support the proposed classification of the observed resonances. Remarkably, the differences between the theoretical and experimental values of the β parameters are large. The analysis of this discrepancy is supported by the results of separate triple coincidence measurements from which main fragmentation mechanisms are deduced. The coincidence measurements consistently indicate a bent geometry of the $S(2p^{-1})\pi^*_{1/2}$ and $S(2p^{-1})\pi^*_{3/2}$ states. [S1050-2947(97)02510-9]

PACS number(s): 33.15.−e, 32.80.Hd, 33.80.Gj

I. INTRODUCTION

High-resolution studies of core-excited molecular levels have recently provided a great deal of information about the structure and the decay dynamics of these states. Thus, for instance, new spectacular effects like ultrafast dissociation from the doubly core-electron excited levels [1] or the breakdown of the spectator decay model [2–4] have been experimentally revealed. Much attention has also been paid to the studies of neutral configurations lying below the core-electron ionization threshold. For a number of diatomic and polyatomic molecules (see, for example, [5,6]) photoabsorption spectra acquired with vibrational resolution have made possible a detailed analysis of single electron core-excited states. However, even in the case of the most thoroughly studied molecules the tentative assignments based on analysis of the Rydberg series have often been questioned in view of results of photoelectron [1] or angular-resolved ion experiments [7]. Especially, the versatility of angular-resolved techniques in identification of molecular states has been shown in several cases [7–9]. Obviously, the most complete picture is obtained by comparing information from various types of experiments.

For this reason we have performed total ion yield and angular-resolved ion yield measurements at the sulfur $2p$ and carbon $1s$ edges of the OCS molecule. By combining these two experimental techniques the results of a quantum defect analysis could be verified by the state symmetry (β-parameter) measurements.

While a standard technique of measuring the total ion yield is typically used to record the absorption structure, various experimental methods such as photoelectron-photoion coincidence (PEPICO) [7], ion kinetic energy [8], or photoion-photoion (PIPICO) measurements [9] have been applied in studies of the anisotropic dissociation following core-electron excitations. Good agreement between theory and experiment has only been obtained for the π^* resonances [8–12], while the dissociation of the Rydberg resonances has been found to be much more isotropic than expected. This discrepancy has remained unexplained until very recently. Precise measurements of the kinetic energy selected ions using a position-sensitive detector have shown that the experimental results and the theoretical predictions converge only if the high kinetic energy ions are taken into consideration [13].

Much less is known about the anisotropic dissociation processes occurring in the core-excited triatomic molecules [14–16]. Actually the interpretation of the results of the β parameter measurements obtained with the triatomic targets is often a difficult task. Even for the rapidly dissociating states the initial orientation of the molecules may be lost if fragmentation occurs via three-body and two-step dissociation processes. Moreover, the geometry of the core-excited state may be bent, in which case the recoil occurs noncollinearly with respect to the molecular orientation. This effect makes the angular orientation of the ejected fragments depend on two parameters: the initial orientation introduced in the absorption process and the angle between the molecular bonds. Actually in simple cases, if one of these parameters is known, the value of the remaining one may be deduced from the data. This approach has recently been applied to the determination of the geometry of the π^* state of the carbon core-electron excited CO_2 molecule [16]. As recently shown [17], the dynamics of three-body processes may be effectively studied using multicoincidence techniques.

In the present work we report vibrationally resolved mea-

surements of the resonant structure in OCS in the vicinity of sulfur $2p$ and carbon $1s$ edges. The anisotropic dissociation following the excitation to these states has been measured in an angular-resolved PEPICO experiment and the β parameters have been separately derived for the C^+, O^+, S^+, CO^+, and CS^+ fragments. The mechanisms leading to total fragmentation and their role for the apparent anisotropy of the C^+, O^+, S^+ fragments are studied in a separate triple electron-ion-ion coincidence (PEPIPICO) measurement. A careful comparison of the obtained data allows for a classification of the core-excited states and a discussion of the dynamics of the excitation and fragmentation processes.

II. EXPERIMENT

The experiment has been performed at beamline 51 at the Swedish National Synchrotron Facility MAX in Lund. The undulator radiation was monochromatized using a modified SX700 monochromator and focused into the interaction region by a refocusing mirror. The polarization degree of the synchrotron light is better than 99% [18]. The bandwidth of the synchrotron light was set to 35 meV at the sulfur $(2p)$ edge and 90 meV at the carbon $(1s)$ edge which is less than the separation of the respective vibrational levels. The synchrotron beam was intersected with a gas jet at right angles and the ambient pressure in the experimental chamber was maintained at 1×10^{-5} mbar. The effective size of the interaction region was less than 2 mm. The measurements were performed with a Wiley-McLaren type of time-of-flight spectrometer (TOF) with 210 mm drift tube length. Both electrons and ions were detected by microchannel plate detectors and the signals were amplified by fast preamplifiers (ORTEC VT 120) and discriminated in a constant fraction discriminator (ORTEC model 935). Coincidence events were acquired with a 2 GHz multihit PC card (FAST model 7886) yielding a time resolution of 0.5 ns. The total ion yield spectra and the PEPIPICO spectra were acquired with high extraction fields (40–50 V/mm) which assured very high collection efficiency. The PEPICO spectra (see Fig. 1) were acquired at the 0°, 90°, and magic angle geometry with low extraction fields (6 V/mm) in order to increase the kinetic energy resolution and angular selectivity. For the same purpose a diaphragm (5 mm diameter) was mounted to the TOF plates in the interaction region. The movement of the synchrotron beam with respect to the TOF during the rotation of the chamber is very small (about 0.1 mm) [18].

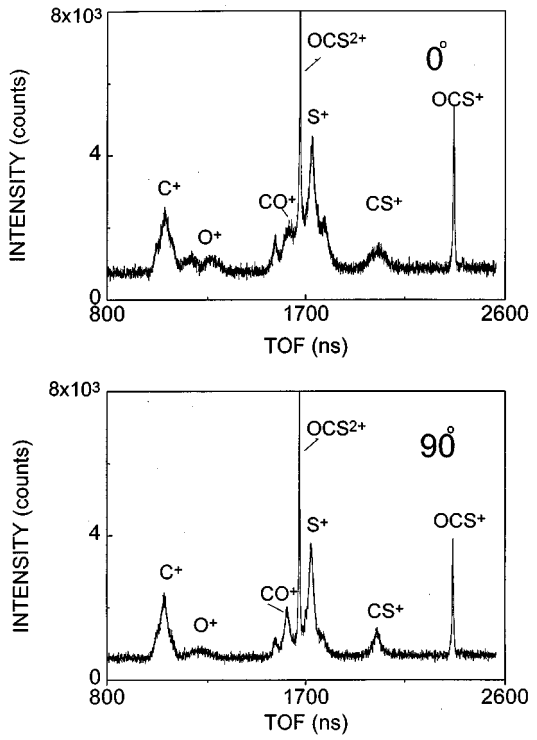

FIG. 1. PEPICO spectra of OCS acquired at the $C(1s^{-1})\pi^*$ resonance at 0° and 90° geometry.

III. EXTRACTIONS OF β PARAMETERS

A. Two-body dissociation from a linear state

For two-body fragmentation processes of triatomic molecules of $C_{\infty v}$ (linear ABC molecule) or $D_{\infty h}$ symmetry the angular distribution of the ejected fragments may be fully described in terms of the asymmetry parameter β. Actually, in such a case, the value of the β parameter should univocally depend on the symmetry of the absorbing state similarly as in diatomic molecules. The discussion of the more general case of fragmentation from the nonlinear states is presented in the next section of this paper. There we will consider qualitatively the role of instantaneous three-body fragmentation and two-step dissociation processes.

In the analysis of the PEPICO spectra we have followed the procedure described in [7]. Briefly, if the kinetic energy distribution [KED, $\chi(v)$] of the produced ions is known, the shape of the PEPICO spectrum in the velocity space may be expressed by the formula

$$S(v_\parallel)=\int_0^{v_{\max}}\chi(v_\perp)P(\alpha(v_\perp,v_\parallel),\beta)dv_\perp, \qquad (3.1)$$

where the function $P(\alpha(v_\perp,v_\parallel),\beta)$ denotes the probability of ejection of the ion under the angle α with respect to the observation axis [$\tan(\alpha)=v_\perp/v_\parallel$, where $v_\perp, v_\parallel$ denote the ion velocity components perpendicular and parallel to the observation axis, respectively]. For an arbitrary observation angle Θ_{obs}, the function P may be calculated by a proper rotation of a probability distribution, which for the observation axis parallel to the polarization plane of the synchrotron radiation $(\Theta_{\text{obs}}=0)$ takes the well-known form

$$P(\alpha,\beta)\propto 1+0.5\beta[3\cos^2(\alpha)-1]. \qquad (3.2)$$

For a given KED distribution, $\chi(v)$, the shape of the $S(v)$ function is solely determined by the anisotropy parameter β. By fitting $S(v)$ to the experimental PEPICO data the β parameter may be found. The advantage of such an approach is that the method is insensitive to the variation of several experimental parameters like intensity of the synchrotron radiation, gas pressure, etc. Although the β parameters may be found from the spectra taken at an arbitrary angle (different from the magic angle), the accuracy of the method increases if results obtained at two very different geometries (preferably 0° and 90°) are simultaneously compared. Certainly, the implicit assumption of an identical value of the β parameters

for all ions considered in the analysis is a serious drawback of the method. From the shape of the PEPICO spectra taken at various angles it becomes obvious that quite often slow ions (kinetic energy $\leqslant 2$ eV) are ejected almost isotropically due to long lifetimes of the respective dissociating states. This effect has been shown in several occasions both in diatomic [8,13] and triatomic [15] molecules. For this reason we have typically excluded ions with kinetic energies $\leqslant 2$ eV from the considerations.

The accuracy of the determination of the β parameter is typically ± 0.1. It should be remembered that the quoted error describes the uncertainty of a ''best fit'' procedure applied to all the recorded ions with kinetic energies higher than 2 eV. The correspondence between the β parameter derived in this way and the real orientation created in the photoabsorption process is good only if the dissociation from all the considered channels occurs faster than the molecular rotation. This certainly needs to be verified by a systematic study of the β parameter dependence on the ion kinetic energy.

The role of the direct ionization processes, which give rise to the approximately constant background level in Figs. 3 and 5, should also be considered. Denoting the cross sections for the direct and the resonant processes by σ_B and σ_R and asymmetry parameters of the background and resonant signal by β_B and β, respectively, the formula for the experimentally measured value β_{expt} reads

$$\beta_{\text{expt}}=\frac{\beta\sigma_R+\beta_B\sigma_B}{\sigma_R+\sigma_B}. \tag{3.3}$$

For the strong resonances Eq. (3.3) has yielded typically 15–25 % correction. At the carbon edge the cross section for direct processes exceeds by almost one order of magnitude the intensity of the Rydberg resonances. In such a case, the realistic estimation of the background signal contribution is difficult mainly due to the somewhat different kinetic energy distributions extracted from the background and resonant spectra as well as the statistical uncertainties, and thus it has not been performed.

As follows from Eq. (3.1) the procedure requires additional measurements of the kinetic energy distribution $\chi(v)$. The $\chi(v)$ functions have been derived for the CS^+, CO^+, C^+, O^+, S^+ ions separately for all the discussed core-excited states from the PEPICO spectra acquired at the magic angle. The deconvolution of the spectra into final KED functions has been described previously [2,3]. We plan to present the results of the analysis of the kinetic energy released in the dissociation of the OCS molecule elsewhere [19].

B. The nonaxial recoil

The two-body fragmentation of the triatomic molecule from the bent state has been described in detail in the original paper of Busch and Wilson [20]. If the molecular rotation may be neglected, the experimentally observed ion distribution $P(\alpha)$ exclusively depends on the initial anisotropy induced in the photoabsorption process and the bent angle of the dissociating molecule. If ψ denotes the angle between the recoil axis and the orientation of the dipole moment, the formula for the measured angular distribution reads

$$P(\alpha)\sim 1+0.5[3\cos^2(\psi)-1][3\cos^2(\alpha)-1]. \tag{3.4}$$

From simple kinematic considerations the relation between the recoil direction and the bond angle may easily be found. Thus, if the degree of orientation of molecules may be estimated, for example, from the known symmetry of the excited state, Eq. (3.4) provides an elegant way of studying the geometry of molecules in core-excited states. Actually, their short lifetimes, causing an overlap of the vibrational structures, make the application of alternative methods difficult.

While the presented formalism may be applied in the analysis of the CO^+ and CS^+ fragments which have been formed in the two-body fragmentation process the results obtained for atomic fragments may be additionally perturbed by three-body (total fragmentation) processes. For example, it has been shown for symmetric molecules (CO_2 [16], CS_2 [17]) that apparent β parameters of the central and terminal atoms may be of the opposite signs. This spectacular effect is observed if the recoil occurs noncollinearly with the main axis of the molecule, e.g., if the molecule is bent. Thus, for equal masses of the terminal atoms, the central fragment gains momentum exclusively in the direction perpendicular to the molecular axis. However, it may be expected that due to large mass difference between the terminal fragments in the OCS molecule, the distribution of the central carbon fragment should be fairly isotropic, since the momentum may also be gained along the intermolecular axis. This makes the information carried by the angular distribution of the carbon fragment less indicative than in the case of symmetric molecules. We discuss the dynamics of the three-body processes of the OCS molecule in the next section. We show that the dominating dissociation mechanism involves a breakup of the OC—S bond and that the production of the C^+ and O^+ fragments mainly occurs via two-step (or quasi-two-step) processes. In such a case the discussed perturbations should weakly affect the shape of the S^+ peak in the PEPICO spectrum, while their importance especially for the C^+ fragments is significant.

IV. RESULTS AND DISCUSSION

A. Total fragmentation processes

Double coincidence measurements may not univocally clarify whether the breakup of the molecule into atomic fragments occurs instantaneously or via two-step dissociations. Since understanding of the kinematics of the occurring processes is crucial for a correct interpretation of β parameter measurements, we have performed separate PEPIPICO experiments from which the dominating fragmentation mechanisms may be deduced.

The PEPIPICO spectra acquired at the excitation energies 164.25 $[S(2p^{-1}\pi^*_{3/2})]$ and 165.51 eV $[S(2p^{-1}\pi^*_{1/2})]$ are shown in Fig. 2 in top and bottom panels, respectively. The observed structure originates from dissociation into $CO^+ + S^+$, $O^+ + S^+ + C$, and $C^+ + S^+ + O$ fragments. As expected [21], the two-body dissociation into the $CO^+ + S^+$ channel appears in the two-dimensional (2D) spectrum as a narrow line tilted at 135° angle. Also the mean slope of the $O^+ + S^+$ coincidence feature is oriented in the same direction, although in this case we observe two diffuse and symmetric spots rather than a line. The large width of these fea-

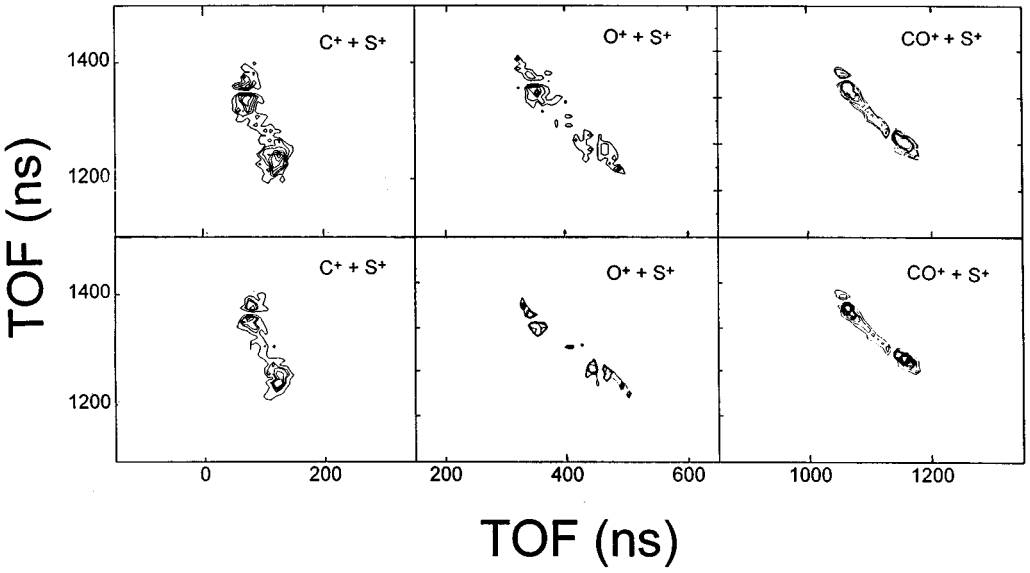

FIG. 2. 2D spectra acquired at the $S(2p^{-1}\pi^*_{3/2})$ (top panel) and $S(2p^{-1}\pi^*_{1/2})$ (bottom panel) resonances. Note the slightly different dispersion of the x and y axes.

tures excludes a pure instantaneous explosion in which the neutral C atom is only a spectator and gains no kinetic energy. Thus the total fragmentation occurs in a rapid sequential process but within the Coulomb zone. In such processes the apparent distribution of the O^+ fragment directly reflects the orientation of the molecules induced in the photoabsorption process only if the geometry of the molecule is linear.

Quite remarkably the shapes of $O^+ + S^+$ 2D spectra recorded at $\pi^*_{1/2}$ and $\pi^*_{3/2}$ resonances are very different. Since the electron deexcitation should occur very similarly (indicating that the dissociation takes place from the same repulsive states), the observed changes should be interpreted in terms of different geometries of the considered states. We will come back to this point later in the paper.

The shape of the $C^+ + S^+$ feature is also characteristic for sequential dissociation preferably occurring with the initial breaking of the OC—S bond. For this reaction the mean slope should be lying between 114° and 135° [21]. The very broad shape of the spectrum indicates that the secondary dissociation is often slow so the orientation is lost due to rotation of the CO^+ fragment. Due to various competing dissociation processes very little anisotropy for the C^+ fragment may be expected.

The 2D data also allow us to estimate the abundance of the S^{2+} ions in the O^+ peak. Since the yield of $S^{2+} + CO^+$ coincidences is more than one order of magnitude weaker than $S^+ + O^+$ coincidences the contribution of the sulfur ions is quite small. It should also be noted that in the 2D spectrum the S^{2+} ions are only observed in coincidence with CO^+. For this reason in further considerations the $m/e = 16$ peak is assigned to O^+. Nevertheless the contribution of the S^{2+} ions may perturb the results of the angular-resolved measurements only if dissociation occurs from a nonlinear state, otherwise the procedure described in the preceding section is applicable to all ions of the same charge-to-mass ratio.

B. The sulfur 2*p* edge

The total ion yield spectrum acquired at the sulfur edge in the energy range 163–183 eV is shown in Fig. 3(a). The details of the complex Rydberg structure are exhibited in Fig. 3(b). The observed resonances originate from transitions to the valence $\pi^*_{3/2,1/2}$ states and to the six Rydberg series converging to the $S(2p^{-1})_{3/2}$ and $S(2p^{-1})_{1/2}$ ionization

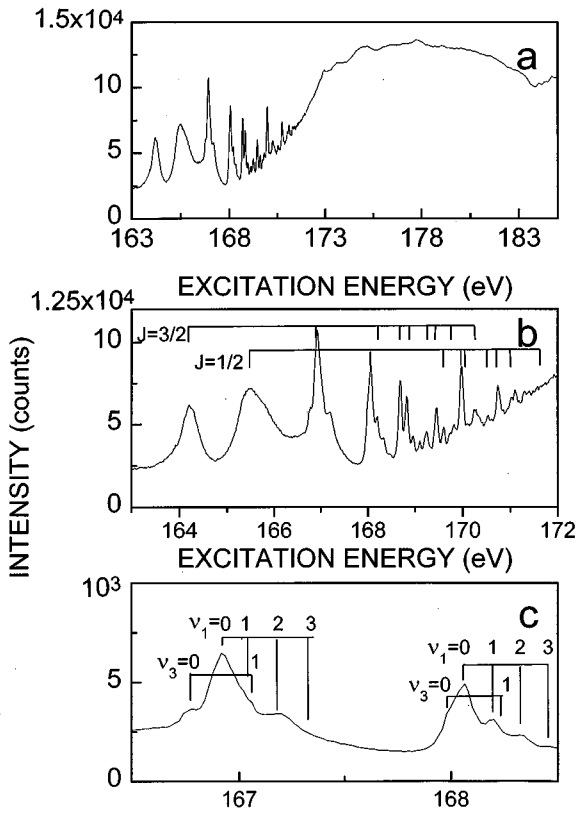

FIG. 3. Total ion yield spectrum acquired at the sulfur edge in the excitation energy ranges 163–183 eV (a), 163–172 eV (b), and 166.5–168.5 eV (c). The vertical bars in (b) correspond to energies of the strongest resonances tabulated in Table I and Table II. In (c) the arrows show the position of the second observed vibrational mode. The bandwidth of the incident light has been set to 35 meV.

TABLE I. Observed energies and derived quantum defects and β parameters of the $J=3/2$ sulfur $2p$ core-electron excited states of the OCS molecule (see Figs. 3 and 4). The accuracy in the β values is ± 0.1.

Energy	State	δ_l	$\beta(CO^+)$	$\beta(CS^+)$	$\beta(C^+)$	$\beta(O^+)$	$\beta(S^+)$
164.25	$\pi^*_{3/2}$		−0.05	0.0	0.0	0.0	0.0
166.94	$4s\,\nu=0$	2.00	0.1	0.2	0.0	0.1	0.2
168.19	$4p$	1.48					
168.71	$3d$	0.11	−0.3	−0.2	−0.2	−0.5	−0.2
168.83	$5s$	1.99					
169.24	$5p$	1.47	−0.2	0.0	0.0	−0.25	0.0
169.43	$4d$	0.11	−0.2	−0.2	−0.1	−0.35	−0.2
169.47	$6s$	2.03					
169.67	$6p$	1.43					
169.76	$5d$	0.11					
169.78	$7s$	2.03					
170.30	L_{III}						

thresholds. The broad $\pi^*_{3/2}$ and $\pi^*_{1/2}$ resonances have been found at 164.2 and 165.5 eV excitation energy, respectively, in good agreement with previous lower-resolution data [22–24]. No vibrational structure of these states has been resolved obviously due to the overlap of the vibrational modes. Below we will show that the geometry of the molecule in the $\pi^*_{1/2,3/2}$ states is bent. The excitation from the linear ground state to a bent state occurs with simultaneous excitation of possible vibrational bending modes (ν_1,ν_2,ν_3) whose fundamental frequencies are in the range 80–250 meV. Although the vibrational separation of each fundamental mode is larger than the instrumental resolution, the overlap of the various vibrational progressions makes the structure impossible to resolve. Similar effects are, for example, observed in the CO_2 molecule [9]. Noticeably, the width of the $\pi^*_{1/2}$ resonance exceeds approximately by a factor of 2 the width of the $\pi^*_{3/2}$ peak, indicating a significant shift of the potential curve of the former level with respect to the ground state (e.g., $\pi^*_{1/2}$ has a broad Franck-Condon region). These peculiar differences between the bond lengths of the LS-split π^* states suggest that strong interactions occur between the excited electron and the remaining core electrons. Apparently this interaction is quite sensitive to the core charge distribution, which is different for the $\pi^*_{1/2}$ and $\pi^*_{3/2}$ states. Since, as we will show below, such differences between the respective Rydberg levels are much less pronounced, the strong interaction only occurs if the ejected core electron is in the compact valence state. Thus the effect may be understood in terms of a strong coupling between the highly localized core hole and the excited electron. Actually our separate measurements [19] reveal a strong localization of the π^* orbital at the sulfur edge, which is exhibited, for example, as a dramatically enhanced (a factor of 10 for the S^{3+} fragment) production of multiply charged sulfur ions in the fragmentation spectra.

In the energy region 166.4–171.5 eV $S(2p^{-1})\ ns_{1/2,3/2}$, $S(2p^{-1})\ np_{1/2,3/2}$, and $S(2p^{-1})\ nd_{1/2,3/2}$ Rydberg series have been resolved and classified (the shorthand notation $nl_{J,J'}$ denotes two states nl_J and $nl_{J'}$, respectively). The tentative assignment of these states based on analysis of the quantum defect is given in Tables I and II. The analysis of the partially resolved vibrational structure of the $4s_{3/2,1/2}$ lev-

TABLE II. Observed energies and derived quantum defects and β parameters of the $J=1/2$ sulfur $2p$ core-electron excited states of the OCS molecule. Note that the values derived for the $3d$ and $4d$ states are perturbed by the overlapping ns resonances (see Figs. 3 and 4). The accuracy in the β values is ± 0.1.

Energy	State	δ_l	$\beta(CO^+)$	$\beta(CS^+)$	$\beta(C^+)$	$\beta(O^+)$	$\beta(S^+)$
165.51	$\pi^*_{1/2}$		−0.25	0.0	−0.1	−0.45	−0.2
168.06	$4s$	2.04	0.25	0.2	0.0	0.6	0.35
169.57	$4p$	1.41					
169.96	$3d$	0.11	−0.3	−0.2	−0.1	−0.25	−0.2
170.02	$5s$	2.07					
170.55	$5p$	1.41					
170.70	$4d$	0.11	−0.2	−0.25	−0.1	−0.25	−0.2
170.74	$6s$	2.03					
170.95	$6p$	1.43					
171.03	$5d$	0.11					
171.05	$7s$	2.03					
171.16	$6p$	1.45					
171.60	L_{II}						

TABLE III. Relative intensities of the vibrational members of the $4s_{1/2,3/2}$ states derived in the multipeak (six Gaussian functions) fitting procedure. The intensity of the ν_3 mode is relative to the intensity of the respective ν_1 mode. Note that the value given for the $4s_{1/2}, \nu_1=1$ state is 20% higher than the intensity of the corresponding $4s_{3/2}, \nu_1=1$ state due to the overlap with the $4p_{3/2}, \nu_1=0$ resonance.

State ν	0	1	2	3
$4s_{3/2}, \nu_1$	1	0.41	0.23	0.07
$4s_{3/2}, \nu_3$	0.46	0.13		
$4s_{1/2}, \nu_1$	1	0.51	0.26	0.06
$4s_{1/2}, \nu_3$	0.28	0.08		

els shows that excitation occurs simultaneously to two vibrational modes (ν_1, ν_3 linear stretching modes) whose intensities differ strongly. Since the separation between these progressions is smaller than the natural width, the first members of the weaker vibrational series ν_3 may only be discerned as shoulders at 166.77 eV and 167.97 eV [Fig. 3(c)]. Up to four members of the ν_1 mode are discernible in the $4s_{1/2,3/2}$ states' spectrum. Since the observed vibrational spacing of the ν_1 mode (130 meV) is very close to its fundamental frequency (111 meV), we may assume that a similar agreement occurs for the ν_3 mode. Under this assumption the experimental spectrum of the $4s_{3/2}$ states may be very well reproduced as a sum of six Gaussian profiles ($\nu_1=0-3$, $\nu_3=0,1$). The relative intensities of the vibrational states found in the multipeak fitting procedure are tabulated in Table III. In the same analysis the natural width of 40 meV of the vibrational states has been found. The same procedure has been applied to the analysis of the $4s_{1/2}$ state and results are also included in Table III. Here the additional difficulty is caused by the accidental superposition of the $4p_{3/2}$, $\nu_1=0$ and the $4s_{1/2}$, $\nu_1=1$ resonances. Higher vibrational members of the $4s_{1/2}$ state are weakly perturbed since the $\nu_1=1$ members of the $4p$ Rydberg progression are very weak. Also at least three vibrational peaks ($\nu_1=0-2$, relative intensities 1:0.35:0.21) are clearly resolved for the $5s_{3/2}$ state. The very weak $\nu_1=3$ is overlapped by the much stronger $5p_{3/2}$ state. The analysis of the vibrational structure of the higher ns Rydberg states leads to rather uncertain results due to their overlap with the members of the nd series.

Interestingly, a very narrow Franck-Condon region has been observed for the excitations to the members of the np series. Although higher Rydberg states coincide in energy with the ns and nd series, distinct members of the np series appear at 169.24 eV ($5p_{3/2}$) and 169.60 ($4p_{1/2}$) excitation energy (Figs. 3 and 4). From the shape of these peaks the $\nu_1=0/\nu_1=1$ ratio has been found to be roughly 7:1 while very weak $\nu_1=2$ levels have not been discerned. This indicates very small changes of the equilibrium distance of the np states and supports our assignment of the vibrational structure at 168.06–168.45 eV mainly to the $4s_{1/2}$ state.

Similarly, no strong excitations to higher vibrational states have been found for the $nd_{1/2,3/2}$ Rydberg series. Although all nd states coincide in energies with the ns resonances, the above may be deduced, for example, from the shape of the $3d_{1/2}$ peak at 169.96 eV for which the contribution of the overlapping $5s_{1/2}$ state is less than 40%. For this

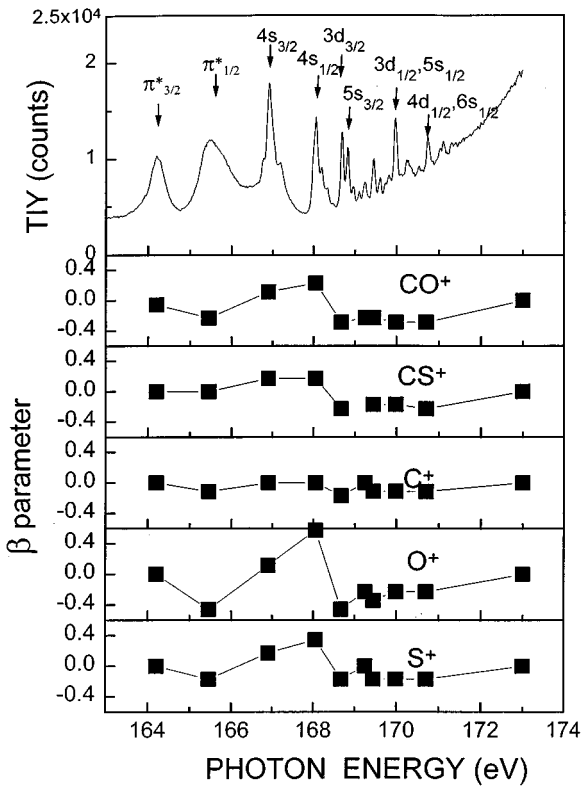

FIG. 4. The β parameters derived for the CO^+, CS^+, C^+, O^+, and S^+ fragments from the PEPICO spectra acquired in the 0° and 90° geometry. Top panel shows the high-resolution total ion yield spectrum measured in the considered energy range.

state only one weak satellite peak has been observed at 170.09 eV which probably originates from the excitation to $5s_{1/2}$ $\nu_1=1$. Moreover, since the regular vibrational progression of the $5s_{3/2}$ state is not apparently perturbed by the neighboring strong $3d_{3/2}$ $\nu_1=0$ resonance the intensities of the $3d_{3/2}$ $\nu_1\leqslant 1$ states are evidently very weak.

The striking variations of the Franck-Condon levels found between members of the Rydberg ns and np, nd series show that the internuclear distances depend strongly on the shape of the Rydberg orbital (e.g., its angular momentum). Not surprisingly a broad Franck-Condon region has been consistently found for the ns states for which the penetration of this Rydberg orbital into the valence shells is large, which is also reflected by a large quantum defect value $\delta\geqslant 2$. The screening effects caused by a Rydberg electron whose orbital is mixed with the valence shell electron weaken the bond strength and give rise to the observed bond length changes. In contrast to the effect observed at the π^* states these variations are not sensitive to the angular momentum of the excited core.

The values of β parameters have been derived following the procedure described in Sec. III for the $\pi^*_{3/2,1/2}$, $4s_{3/2,1/2}$, $3d_{3/2,1/2}$, $4d_{3/2,1/2}$, and $5p_{3/2}$ resonances. The results are included in Tables I and II, and displayed in Fig. 4. While the C^+ fragments show little variation of the β parameter, a range of $-0.5-0.3$ has been found for the remaining fragments.

Clearly (see Fig. 4) the β parameter observed for the $\pi^*_{3/2}$ and $\pi^*_{1/2}$ states differ strongly. While the dissociation from

TABLE IV. Observed energies and derived β parameters of the carbon $1s$ core-electron excited states of the OCS molecule (see Fig. 5). The accuracy in the β values is ± 0.1.

State	Energy	δ_l	$\beta(CO^+)$	$\beta(O^+)$	$\beta(S^+)$
$\pi^*, \nu_1=0$	288.33		−0.6	−0.3	−0.2
$\pi^*, \nu_1=1$	288.53				
$\pi^*, \nu_1=2$	288.73				
$\pi^*, \nu_1=3$	288.93				
$3s\,\nu_1=0$	291.30	1.21	0.2	0.1	0.1
$3p\,\nu_1=0$	291.82	1.09	0.0	0.0	−0.1
$3d\,\nu_1=0$	293.15	0.60			
$4s\,\nu_1=0$	293.76	1.21			
$4p\,\nu_1=0$	293.90	1.09	0.0	0.0	−0.1
$5p\,\nu_1=0$	294.60	1.09			
$C(1s^{-1})$	295.50				

the latter resonance is strongly anisotropic, clearly showing the π character of the excited states, the fragmentation from the former state yields $\beta=0$ for all the analyzed fragments. Since we do not expect dramatic differences in the deexcitation mechanism of the $\pi^*_{1/2}$ and $\pi^*_{3/2}$ states and no such changes have been observed in the extracted kinetic energy distributions, a loss of the orientation due to molecular rotation should be ruled out from the considerations. Alternatively, the anisotropy may be smeared out if the geometry of the π^* states is bent. The nonlinearity of the π^* state would also explain the very dense vibrational structure of these states found in the total ion yield spectra and the very different shapes of the $O^+ + S^+$ coincidence feature recorded in the 2D spectra at the two resonances (see Fig. 2). Assuming that the excitation to the π^* states is a pure Σ-Π type transition the bent angle may be estimated from Eq. (3.4). The obtained values are 140° and 132° for the $\pi^*_{1/2}$ and $\pi^*_{3/2}$ states, respectively.

The values of the β parameters extracted for the $4s_{3/2}$ and $4s_{1/2}$ states are consistently positive for all the analyzed fragments, indicating the σ symmetry of the excited state. They are remarkably different, probably due to much stronger excitations to the vibrational bending modes occurring for the transition to the $4s_{3/2}$ state. The β parameters obtained for the analyzed nd and np Rydberg states are slightly negative in accordance with the assigned π symmetry of the transitions. The discrepancy between the measured β parameters and the values expected for transitions of a pure Σ-Σ or Σ-Π symmetry may partially be explained by the overlap nd levels with the ns series which causes a mixing of the π and σ types of orientation. Also for the weak states ($5p_{3/2}$, $6s_{1/2}$) the error introduced by the background signal becomes significant.

It is quite striking that the largest asymmetry parameters have been found for the O^+ fragment. This observation is in agreement with the conclusions of the 2D data analysis presented in Sec. IV A. Also the shapes of the coincidence maps suggest that the anisotropy of the C^+ fragment is lost in the two-body dissociation. Clearly the differences in measured β parameters for the O^+ and C^+ fragments are mainly due to their different kinetic energies. This seems to indicate that the experimental and theoretical values of the β parameters may converge with increasing kinetic energy of the analyzed ions.

C. The carbon 1s edge

The total ion yield spectrum acquired in the energy range 287–296 eV is shown in Fig. 5 (top panel). The energies, assignments, and calculated quantum defects of the resolved states are tabulated in Table IV. Four vibrational levels separated by 205 meV may be distinguished in the π^* peak spectrum (288 eV excitation energy). By fitting a multipeak Gaussian function the relative intensities of the vibrational resonances have been determined to 1:0.62:0.28:0.084 for $\nu_1=0,1,2,3$, respectively, and their natural width has been found to be about 130 meV. No additional vibrational modes have been observed, suggesting a linear configuration of the molecule in the $C(1s^{-1})\pi^*$ state. Five Rydberg states have been discerned at 291.30 eV, 291.82 eV, 293.15 eV, 293.90 eV, and 294.60 eV photon energy, and identified as $3s$, $3p$, $3d$, $4p$, and $5p$ resonances, respectively. The $4s$ state is separated from the much stronger $4p$ resonance by 0.2 eV and it is therefore observed only as a weak shoulder at the $4p$ peak. Noticeably, the intensity of all the resonances is 3–7 times weaker than the background level. Although the vibrational members of the $3s$, $3d$, $3p$, and $4p$ states have not been directly resolved, the small differences in their widths reveal somewhat unequal Franck-Condon factors for excitation to these states. Clearly these differences are much smaller than those found for the sulfur core-excited states, which shows a much weaker role of the carbon core-excited Rydberg electron in formation of the bonding states.

Above the $5p$ resonance a number of unresolved ns and np Rydberg states form a broad feature which spans up to the ionization threshold at 295.5 eV. The comparison of the intensities of the $3s$, $3d$, and $3p$ states shows that the total contribution of the ns, nd states to the considered feature is much weaker than that of the respective np states.

The derived β parameters for the O^+, S^+, and CO^+ fragments have been extracted from the PEPICO data and results are included in Table IV and shown in Fig. 5. The intensities of the CS^+ fragments are very weak, making the analysis of the anisotropy parameter of this fragment difficult. Also for the C^+ fragments released with low kinetic energy the observed distribution is almost isotropic and is not shown.

The β parameters extracted at the π^* resonance for the CO^+, O^+, and S^+ analyzed fragments are negative as ex-

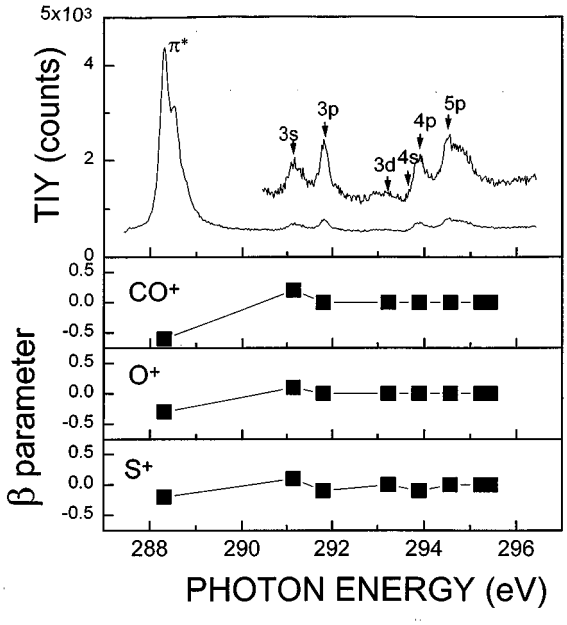

FIG. 5. Total ion yield spectrum acquired at the carbon edge (top panel, bandwidth 90 meV) and the derived β parameters for the CO^+, O^+, S^+ fragments.

pected, although the deviation from the theoretical value is large except for the CO^+ fragment. This is not surprising since this distribution is not perturbed by possible three-body processes as is the case of the remaining O^+ and S^+ fragments. In the Rydberg series region some anisotropy has been found at the 3*s* state while *np* resonances reveal only very weak π character. Similar isotropic distributions have been found at the threshold region for all the fragments. This may partially be explained by the dominating contribution of the background signal measured in the PEPICO spectrum although the results suggest a much weaker degree of anisotropy for excitations to the higher Rydberg levels. For the previously mentioned reasons the extraction of the background signal leads to rather uncertain results and has not been performed in this case.

V. CONCLUSIONS

We present studies of the sulfur and carbon core-electron singly excited states based on high-resolution total ion yield and angular-resolved coincidence measurements. The analysis of the total ion yield spectra allows for the assignment of the resonant structure in terms of single electron transitions to valence and Rydberg levels of the neutral OCS molecule. The relative intensities of the vibrational levels indicate significant bond length changes for the core-electron excitations to the various valence and Rydberg states. This effect is very pronounced for the sulfur core-electron excited states and suggests strong interactions between the localized hole and the excited electron.

From the PEPICO spectra acquired at 0° and 90° geometry the β parameters have been extracted independently for the various energetic fragments. Although the extracted β values are in accordance with the assignment deduced from the analysis of the Rydberg progressions, the discrepancy between the measured and expected values is in general large. For the sulfur core-excited π^* states both total ion yield and angular-resolved measurements suggest a bent geometry of these states. Assuming a negligible role of the molecular rotation we have derived respective bent angles from the measured β parameters.

[1] M. Neeb, A. Kivimäki, B. Kempgens, H. M. Köppe, J. Feldhaus, and A. M. Bradshaw, Phys. Rev. Lett. **76**, 2250 (1996).
[2] P. Erman, A. Karawajczyk, U. Köble, E. Rachlew-Källne, and K. Yoshiki-Franźen, Phys. Rev. A **53**, 1407 (1996).
[3] P. Erman, P. Hatherly, A. Karawajczyk, U. Köble, E. Rachlew-Källne, M. Stankiewicz, and K. Yoshiki-Franźen, J. Phys. B **29**, 1501 (1996).
[4] E. Kukk, H. Aksela, O.-P. Sairanen, E. Nommiste, S. Aksela, S. J. Osborne, A. Ausmees, and S. Svensson, Phys. Rev. A **54**, 2121 (1996).
[5] Y. Ma, C. T. Chen, G. Meigs, K. Randall, and F. Sette, Phys. Rev. A **44**, 1848 (1991).
[6] G. Remmers, M. Domke, A. Puschmann, T. Mandel, and G. Kaindl, Chem. Phys. Lett. **214**, 241 (1993).
[7] N. Saito and I. H. Suzuki, Phys. Rev. Lett. **61**, 2740 (1988).
[8] A. Yagishita, H. Maezawa, M. Ukai, and E. Shigemasa, Phys. Rev. Lett. **62**, 36 (1989).
[9] J. D. Bozek, N. Saito, and I. H. Suzuki, J. Chem. Phys. **100**, 393 (1994).
[10] K. Lee, D. Y. Kim, L. I. Ma, D. A. Lapiano-Smith, and D. M. Hanson, J. Chem. Phys. **93**, 7936 (1990).
[11] O. Hemmers, F. Heiser, J. Eiben, R. Wehlitz, and U. Becker, Phys. Rev. Lett. **71**, 987 (1993).
[12] E. Shigemasa, K. Ueda, Y. Sato, T. Sasaki, and A. Yagishita, Phys. Rev. A **45**, 2915 (1992).
[13] N. Saito, F. Heiser, O. Hemmers, K. Wieliczek, J. Viefhaus, and U. Becker, Phys. Rev. A **54**, 2004 (1996).
[14] D. Y. Kim, K. Lee, C. I. Ma, M. Mahalingam, D. M. Hanson, and S. L. Hubert, J. Chem. Phys. **97**, 5915 (1992).
[15] J. D. Bozek, N. Saito, and I. H. Suzuki, J. Chem. Phys. **98**, 4652 (1993).
[16] J. D. Bozek, N. Saito, and I. H. Suzuki, Phys. Rev. A **51**, 4563 (1995).
[17] M. Simon, M. Lavollée, M. Meyer, and P. Morin, J. Electron Spectrosc. Relat. Phenom. **79**, 401 (1996).
[18] H. Aksela, J. Jauhiainen, E. Nommiste, S. Aksela, S. Sundin, A. Ausmees, and S. Svensson, Phys. Rev. A **54**, 605 (1996).
[19] P. Erman, A. Karawajczyk, E. Rachlew-Källne, M. Stankiewicz, and K. Yoshiki Franźen (unpublished).
[20] G. E. Busch and K. R. Wilson, J. Chem. Phys. **56**, 3626 (1972).
[21] J. H. D. Eland, Mol. Phys. **61**, 725 (1987).
[22] A. A. Krasnoperowa, E. S. Gluskin, and L. N. Mazalov, J. Struct. Chem. **18**, 206 (1977).
[23] T. K. Sham, B. X. Yang, J. Kirz, and J. S. Tse, Phys. Rev. A **40**, 652 (1989).
[24] G. R. Wright and C. E. Brion, J. Electron Spectrosc. Relat. Phenom. **4**, 335 (1974).